

## Signatures of Kelvin and Rossby wave propagation in the northern Indian Ocean from TOPEX/POSEIDON Altimeter

S. Prasanna Kumar, A.S. Unnikrishnan and P.M. Muraleedharan  
National Institute of Oceanography, Dona Paula, Goa-403 004, India  
E-mail: prasanna@csnio.ren.nic.in

### Abstract

The climatological monthly mean sea surface height (SSH) anomalies derived from T/P altimeter in the northern Indian Ocean, during 1993 to 1997, are used to prepare time-longitude plots. Along the equator they reveal strong semi-annual variability of sea level anomaly. The plots along 6°, 12° and 18°N show the westward propagating (Rossby waves) features, the speed of which decreases from 7.74 cm s<sup>-1</sup> at 12°N to 4.50 cm s<sup>-1</sup> at 18°N. These speeds are comparable to the theoretical phase speeds of Rossby waves. Time-longitude plots of zonal wind stress, obtained from the FSU wind stress climatology for the same period as that of T/P data, shows that the eastward propagation in the sea level field in the equatorial region is driven by zonal wind stress variability, whereas the westward propagation in the higher latitudes is found to have little influence with the zonal wind stress variability. Moreover, it is found that the westward propagation of high (low) sea level anomaly along 12°N in the Arabian Sea appears to be driven by the Ekman convergence (divergence) associated with the negative (positive) wind-stress curl near the southern tip of the peninsular India and Sri Lanka between 5 and 10°N.

### 1. Introduction

Northern Indian Ocean comprises of two tropical basins, the Arabian Sea and the Bay of Bengal. One of the characteristic features of this ocean is the presence of both annual and semi-annual periodicity. During summer monsoon (June to September) southwesterly winds (~ 15 m s<sup>-1</sup>) prevail in the northern Indian Ocean while during winter monsoon (November-February) winds are northeasterly (~ 5 m s<sup>-1</sup>). It is generally understood that large-scale forcing associated with the monsoon winds generate eastward propagating Kelvin waves along the equator which get reflected at the eastern boundary and propagate westward as Rossby waves, and also as coastally trapped Kelvin waves along the eastern periphery. These Kelvin and Rossby waves are important dynamic features of the equatorial ocean, as they are capable of transferring wind energy from one end of the ocean basin to the other end due to their non-dispersive character.

Numerical models have shown the role of these waves in the dynamics of the northern Indian Ocean (Potemra, 1991; Yu et al., 1991; McCreary et al., 1993). An analysis of temperature climatology (Prasanna Kumar and Unnikrishnan, 1995; Unnikrishnan et al., 1997) has shown the characteristics of the westward propagating Rossby waves in the Bay of Bengal. A major constraint in the study of such large-scale, low-frequency variability is the non-availability of data having sufficient spatio-temporal resolution. With the advent of satellite technology and remote sensing technique, it is now becoming increasingly possible to address this.

A recent study of Eigenheer and Quadfasel (2000), with the help of altimeter data, indicated that the variability associated with the circulation in the interior Bay of Bengal and particularly, the east India coastal current is influenced by the remotely forced planetary waves. In this article, the signatures of Kelvin and Rossby waves in the northern Indian Ocean were deciphered using sea level anomalies from TOPEX/POSEIDON (T/P) altimeter data.

### 2. Data

The T/P altimeter data used in this study were the gridded sea level anomalies, computed from conventional repeat-track (collinear difference) analysis of T/P GDR (geophysical data record), for each 10-day repeat cycle. The spatial resolution of the data is 0.25° longitude by 0.25° latitude (AVISO User Handbook, 1997). From the global data, the data for the northern Indian ocean between longitudes 40°E to 100°E and latitudes north of 10°S covering the period 1993 to 1997 were utilised in the present study to prepare monthly mean climatologies. Similarly, monthly mean FSU winds during the same period were used to construct climatologies of zonal and meridional components of wind-stress and for the computation of wind-stress curl.

### 3. Results and Discussion

In order to decipher the features of propagation, time-longitude variation of sea level anomalies along different latitudes (equator, 6°, 12° and 18°N) were plotted (Fig. 1-3 & 5).

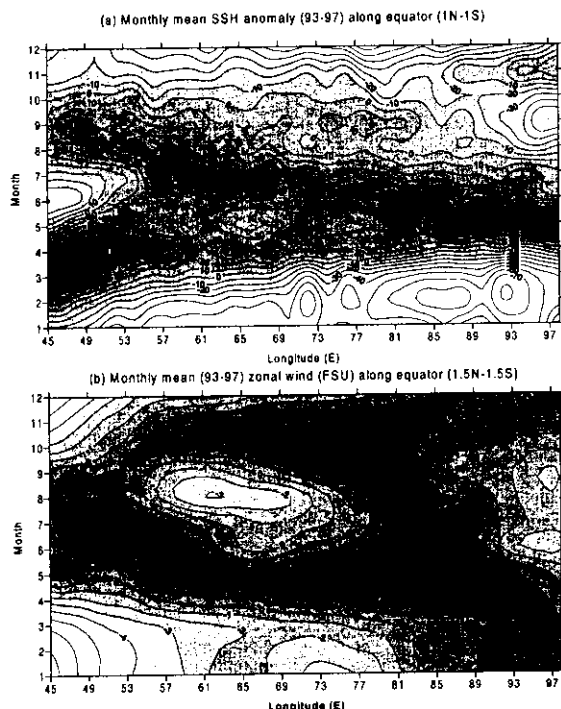


Fig. 1 Time-longitude plot of monthly mean (1993-97) (a) SSH anomaly and (b) FSU zonal wind along the equator. Shaded region in (a) indicates high sea level while that in (b) is westerly wind. SSH anomalies are averaged within one degree while FSU winds are averaged over 1.5 degree north and south of the equator.

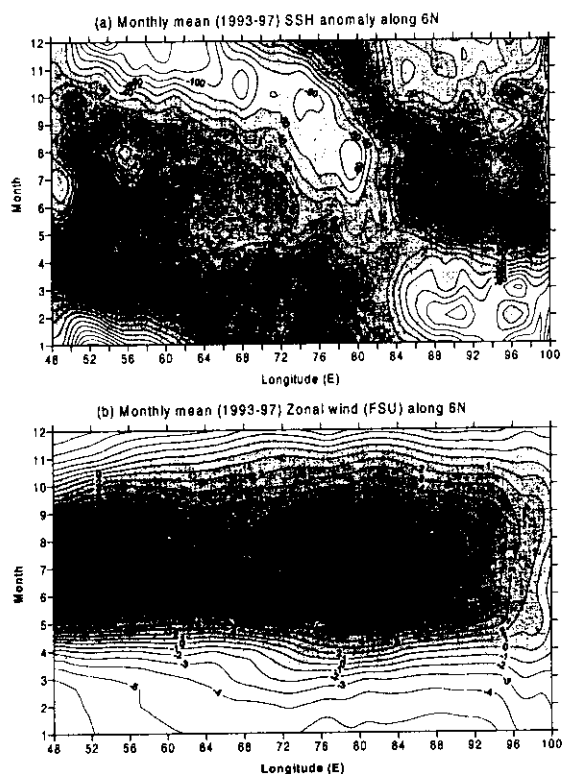


Fig. 2 Time-longitude plot of monthly mean (1993-97) SSH anomaly and (b) FSU zonal wind along 6°N. Shaded region in (a) indicates high sea level while that in (b) is westerly wind.

The sea level anomalies along the equator (averaged within 1 degree on either side of the equator) reveal strong semi-annual sea level variability in the western and eastern parts of the equator (Fig. 1a). The high in the sea level field during March and September generates eastward propagating Kelvin waves in the equatorial region (Fig. 1a). This is more conspicuous during March, when the eastward sloping isolines indicate Kelvin wave propagation. The high in the sea level field, which appears near the western equatorial region, takes about two months to reach the eastern boundary, giving a propagation speed of about  $1.12 \text{ m s}^{-1}$ . Earlier, based on the climatological temperature distribution for the Bay of Bengal, Prasanna Kumar and Unnikrishnan (1995) deduced the speed of the equatorial Kelvin wave to be  $1.0 \text{ m s}^{-1}$ , which is weaker but consistent with the theoretical speed. A look at the zonal winds along the equator (Fig. 1b, averaged over 1.5 degree on either side of the equator) reveals that the strength of the easterly winds progressively decreases and become westerly by March in the eastern region. Westerly winds become fully established by April in the central and eastern equatorial regions. Again by September, organised westerly winds start appearing in the central and eastern region of the equator. Thus, the high SSH field during March and September seems to be generated by zonal wind.

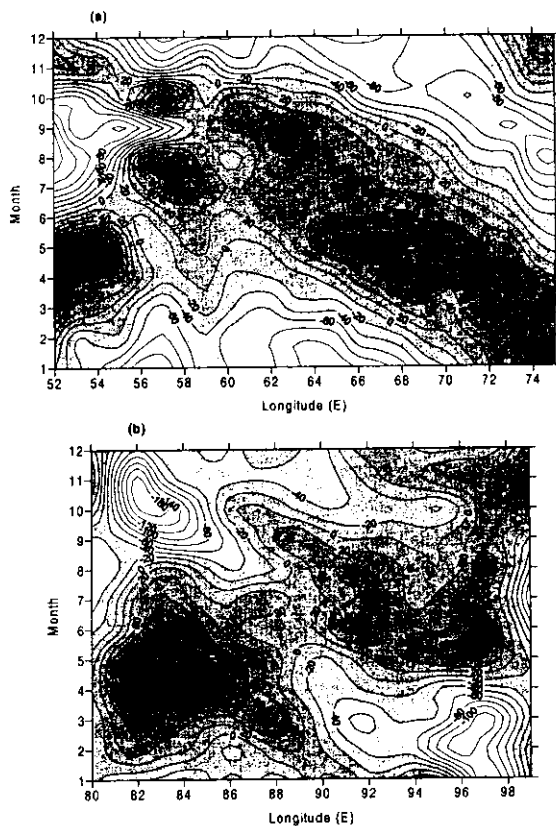


Fig. 3 Time-longitude plot of monthly mean (1993-97) SSH anomaly along 12°N in the (a) Arabian Sea and (b) Bay of Bengal. Shaded region indicates high sea level.

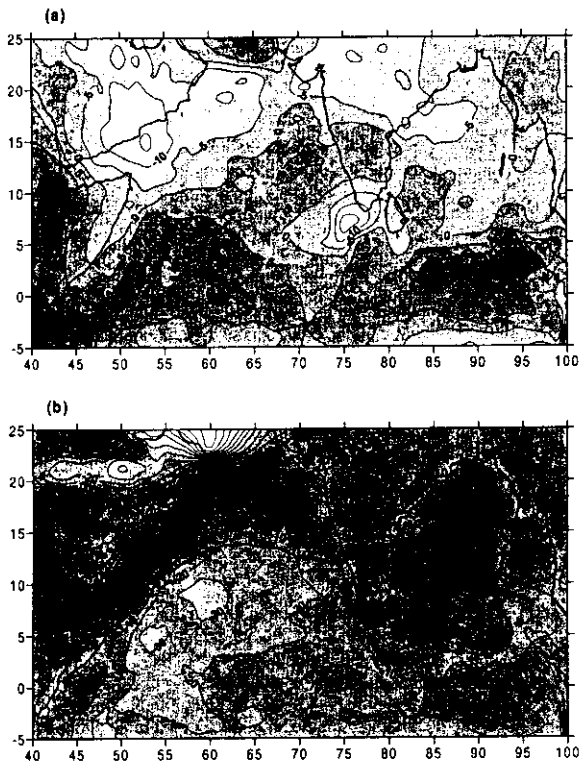


Fig. 4 Monthly mean (1993-97) wind-stress curl ( $\times 10^{-6} \text{ Pa m}^{-1}$ ) for (a) January and (b) July. Note the change in contour interval in (b).

Along  $6^\circ\text{N}$ , low sea level anomaly seen in the eastern region during February reaches the western boundary by December (Fig.2a). The sloping contours indicate the signatures of westward propagating Rossby waves. Time evolution of the zonal wind along this latitude shows that during April to October winds are eastward, with its peak from June to September, while during rest of the year it is westward (Fig.2b). A comparison of the sea level anomaly and the zonal wind reveals that the westward propagation of low sea level is in phase with the easterly zonal winds during January to March, though its strength progressively decreases, but is strongly countered by the strengthening westerly winds till October. Once again from November zonal winds are easterly, in phase with westward propagating sea level. In short, from the above it would seem that the westward propagation of low sea level is independent of the seasonal reversal of zonal winds.

Along  $12^\circ\text{N}$ , in the Bay of Bengal a low sea level anomaly seen in March near the eastern region moves westward and reaches the western boundary in mid October (Fig.3b). Interestingly, in the Arabian Sea, a high sea level anomaly is seen near the eastern region in January and it moves westward (Fig.3a). The low sea level seen in July near the western boundary is associated with Somali upwelling. The offshore advection of cold upwelled water from the Somali upwelling region appears to limit the westward propaga-

tion of high sea level anomaly at this time of the year. This upwelling signature persists till October, as indicated by the low sea level anomaly. From the eastern region of the Bay of Bengal, a low sea level moves westward during May and reaches the western boundary by February. Time evolution of zonal wind at this latitude for both the Bay of Bengal and the Arabian Sea (not presented) is similar to that at  $6^\circ\text{N}$ . Once again the westward propagation appears to be not related to the zonal wind distribution at this latitude. A look at the distribution of wind-stress curl (Fig.4a, for January) shows a negative curl near the southern tip of the peninsular India and Sri Lanka between  $5$  and  $10^\circ\text{N}$  which appears in November, peaks in January and decays in February. This negative wind-stress curl produces a high sea level, which propagates westward as noticed in the time-longitude plot (Fig.3a). From May onwards a positive wind-stress curl replaces the negative curl in this region which persists till September (Fig.4b, for July). Ekman divergence associated with it produces low sea levels which propagates westward as seen in Fig. 3a.

Along  $18^\circ\text{N}$ , in the Bay of Bengal, the dominant feature is the westward moving low sea level which takes

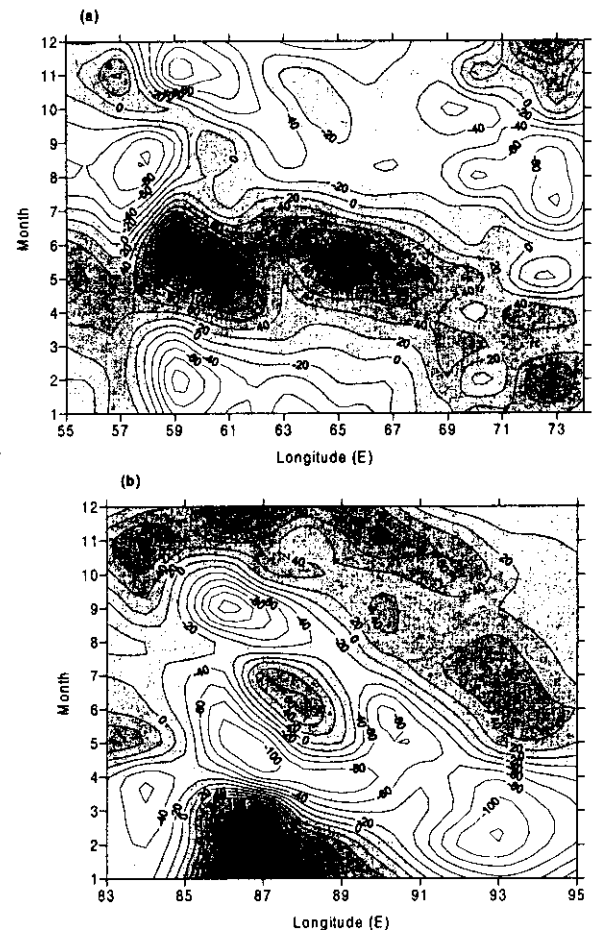


Fig. 5. Time-longitude plot of monthly mean (1993-97) SSH anomaly along  $18^\circ\text{N}$  in the (a) Arabian Sea and (b) Bay of Bengal.

about 9 months to travel from east to west (Fig.5b). In the Arabian Sea such a propagation is not seen (Fig.5a). However, in January, a high sea level appears to move offshore from the eastern region. During July to September, the low sea level seen close to western boundary is the signature of coastal upwelling along Arabia. Interestingly, most of the open ocean region is occupied by the low SSH anomaly during this time of the year. Again the time evolution of the zonal wind at this latitude (not presented) is similar to that of 6°N. A look at the distribution of the wind-stress curl (Fig. 4b) during July reveals that along 18°N wind-stress curl is positive. The low sea level, noticed during June to September in the central Arabian Sea, is the manifestation of open sea upwelling driven by Ekman divergence associated with the positive wind-stress curl. Incidentally, the climatological mean position of wind speed maximum associated with the Findlater jet, which becomes active during June to September, lies at around 63-64°E in this latitude. The low sea level during summer monsoon along the coast of Arabia extends into the central Arabian Sea (up to 65°E) due to lateral advection of upwelled cold water as well as the open ocean upwelling, the latter driven by the positive wind-stress curl north of the Findlater jet (Bauer, 1991). Near the eastern boundary, the low sea level during summer is associated with the upwelling along the west coast of India.

We computed the phase speed of free Rossby waves (Gill, 1982) taking reduced gravity as 0.0369 and equivalent depth as 120 m. Theoretical phase speed thus obtained compares well with that obtained from SSH anomaly (Table 1).

**Table 1.** Computed and theoretical phase speed of westward propagating Rossby wave (first baroclinic mode for a two-layer ocean) at different latitudes.

Latitude (N)	Computed speed from SSH anomaly (cm s <sup>-1</sup> )	Theoretical phase speed (cm s <sup>-1</sup> )
12	7.74	9.54
18	4.50	4.33

From the above results, it is evident that the upper ocean variability of the Bay of Bengal, to a large extent, is controlled by the westward propagating Rossby waves. However, in the Arabian Sea, westward propagation from the peninsular India influences the variability in the southern parts, whereas in the central and northern regions, local forcing controls it. We plan to study the effect of local and remote forcing on the circulation of the two basins in detail.

### Acknowledgement

We thank James N. Stricherz, for making available the FSU winds for Indian Ocean region. This is NIO contribution 3586.

### References

- AVISO, 1997, *AVISO User Handbook - Sea level anomalies*, Rep.AVI-NT-011-312-CN, Edition 3.0, CNES, Toulouse, France, 24 pp.
- Bauer, S., G.L. Hitchcock and D.B. Olson. 1991. Influence of monsoonally forced Ekman dynamics of upper surface layer depth and phytoplankton biomass distribution in the Arabian Sea. *Deep-Sea Res.*, 38, 531-553.
- Eigenheer, A. and D. Quadfasel, 2000, Seasonal variability of the Bay of Bengal Circulation inferred from TOPEX/Poseidon altimeter, *J. Geophys. Res.*, 105, 3243-3252.
- Gill, A.E., 1982, *Atmosphere-Ocean Dynamics*, San Diego, Calif., Academic, 662 pp.
- McCreary, J.P., P.K. Kundu, and R.L. Molinari, 1993, A numerical investigation of dynamics, thermodynamics and mixed-layer processes in the Indian Ocean, *Prog. Oceanogr.*, 31, 181-244.
- Potemra, J.E., M.E. Luther, and J.J. O'Brien, 1991, The seasonal circulation of the upper ocean in the Bay of Bengal, *J. Geophys. Res.*, 96, 12,667-12683.
- Prasanna Kumar, S., and A.S. Unnikrishnan, 1995, Seasonal cycle of temperature and associated wave phenomena in the upper layers of the Bay of Bengal, *J. Geophys. Res.*, 100, 13,585-13,593.
- Unnikrishnan, A.S., S. Prasanna Kumar, and G.S. Navelkar, 1997, Large-scale processes in the upper layers of the Indian Ocean inferred from temperature climatology, *J. Mar. Res.*, 55, 93-115.
- Yu, L., J. J. O'Brien, and J. Yang, 1991, On the remote forcing of the circulation in the Bay of Bengal, *J. Geophys. Res.*, 96, 20,449-20,454.